Quantum-Field-Theory Approach to the Heisenberg Ferromagnet*†

H. J. SPENCER

Solid-State Theory Group, Department of Physics, Imperial College, London, England

(Received 10 July 1967)

Earlier derivations of simple Wick's theorems for operators of spin $\frac{1}{2}$ and 1 (in units of $\hbar$) using the drone-fermion representation are applied to the Heisenberg model. The resulting diagrammatic-perturbational approach (Green's functions) is carried out in both the high- and low-temperature domains, where the expansion criteria of Stinchcombe *et al.* are closely followed. The present work effectively reexpresses the semi-invariant analysis of these authors in a much simpler manner, and many of their results are straightforwardly reproduced. The use of standard quantum-field-theory techniques enables renormalization to be undertaken in a simple, systematic manner. At low temperatures the present fermion analysis gives Dyson's T^4 contribution to the free energy from the first Born approximation to spin-wave scattering. Higher-order spin-wave contributions give a damping term, which, upon evaluation in the lowest approximation, is identical to that found by ter Haar and Tahir-Kheli.

1. INTRODUCTION

IN this paper the powerful techniques of quantum-field theory[1] are systematically applied to the Heisenberg model, which has been the focus of spin problems for over 30 years.[2] Previously, these methods could not be used because of the absence of a Wick-like theorem[3] for manipulating products of spin operators. This obstacle has been overcome by the author in two earlier papers,[4] for the two cases of $S=\frac{1}{2}$ and $S=1$, using the drone-fermion representation of the spin operators. Before proceeding with the present method, a brief summary of earlier work would be useful to establish the context of the present paper among such diverse approaches.

Dyson[5] first gave a rigorous theory of the low-temperature thermodynamic behavior of this model when (*inter alia*) he justified spin-wave theory at low temperatures and showed that spin-wave scattering effects are negligible as the temperature goes to zero. This work provided the theoretical justification for the neglect of the so-called kinematic effects in this temperature regime for many subsequent theories, such as Oguchi's[6] approach via the Holstein-Primakoff transformation[7] of the spin operators. This low-temperature justification of spin-wave theory will again be demonstrated in Sec. 3 from first principles. Bloch[8] used the Holstein-Primakoff transformation to retain all the diagonal terms in the Hamiltonian up to 4th order in the resulting annihilation and creation operators. The validity of this approximation was assumed through the whole temperature range, to give the spin-wave renormalization results by a self-consistent calculation, using a variational argument on the free energy. Szaniecki,[9] in a series of papers, approached this problem starting from Dyson's (equivalent) boson Hamiltonian at low temperatures and then using quantum-field-theory techniques for a diagramatic boson analysis of the free energy.

A new approach was taken by Tahir-Kheli and ter Haar,[10] using double-time temperature Green's functions. In their first paper, the decoupling procedure of Bogolyubov and Tyablikov[11] for $S=\frac{1}{2}$ was generalized to all S, although explicit results were only presented up to $S=3$, because of the increasing complexity of their equations. In a second paper, the Green's functions resulting from Dyson's Hamiltonian were decoupled, giving the spin-wave renormalization obtained by Brout and Englert,[12] and a higher-order decoupling resulted in a damping coefficient in the spin-wave energies. In a certain approximation these results are recovered in Sec. 4. Callen[13] developed (using $S=\frac{1}{2}$ as a guide) a method for solving the equations resulting from his decoupling approximation to the equations of motion for general spin-operator averages. Unfortunately, this introduced a spurious T^3 error in his results for $S=\frac{1}{2}$ but not for higher S. However, Morita and Tanaka,[14] by extending the decoupling scheme for $S=\frac{1}{2}$ to the next order and using an analogy based on

† S.R.C. postdoctoral fellow.

* These results have arisen during the preparation of a Ph.D. thesis to be submitted to the University of London.

[1] A. A. Abrikosov, L. P. Gorkov, and I. Ye. Dzyaloshinskii, *Quantum Field Theoretical Methods in Statistical Physics* (Pergamon Press, Inc., New York, 1965).

[2] F. Bloch, Z. Physik **61**, 206 (1930); **74**, 295 (1932).

[3] G. C. Wick, Phys. Rev. **80**, 268 (1950).

[4] H. J. Spencer, Phys. Rev. (to be published).

[5] F. J. Dyson, Phys. Rev. **102**, 1217 (1956); **102**, 1230 (1956).

[6] T. Oguchi, Phys. Rev. **117**, 117 (1960).

[7] T. Holstein and H. Primakoff, Phys. Rev. **58**, 1098 (1940).

[8] M. Bloch, J. Appl. Phys. **34**, 1151 (1963).

[9] J. Szaniecki, Acta Phys. Polon. **21**, 3, 219 (1962); **22**, 379 (1963); **22**, 381 (1963).

[10] R. A. Tahir-Kheli and D. ter Haar, Phys. Rev. **127**, 88 (1962); **127**, 95 (1962).

[11] N. N. Bogolyubov and S. V. Tyablikov, Dokl. Akad. Nauk, SSSR **126**, 53 (1959) [English transl.: Soviet Phys.—Doklady **4**, 589 (1959)].

[12] R. Brout and F. Englert, Bull. Am. Phys. Soc. **6**, 55 (1961).

[13] H. B. Callen, Phys. Rev. **130**, 890 (1963).

[14] T. Morita and T. Tanaka, Phys. Rev. **137**, A648 (1965).

the exactly soluble two-spin problem, were able to obtain the famous Dyson T^4 contribution to the magnetization at low temperatures. This is also obtained in Sec. 4 of the present paper.

Haas and Jarrett[15] attempted to unify these Green's-function theories and also that of Bloch by a generalized form of the decoupling approximation, involving two variable parameters chosen to give the original expressions for the magnetization. However, in all such equations-of-motion methods the justification of the actual decoupling chosen is always *a posteriori*, rather than *a priori*, as in the approximations used in other theories.

All the above-mentioned methods have concentrated on the low-temperature or spin-wave region. The work of Englert,[16] Brout,[17] Stinchcombe *et al.*,[18] and Lewis and Stinchcombe,[19] amongst others, has resulted in theories which are applicable in both the high- and low-temperature domains. The present work fits into this category. In fact, the present work is a fermion Green's-function theory, which bears a very close similarity to the quantum-mechanical semi-invariants introduced by Stinchcombe *et al.*, and it effectively introduces dynamical substructure into their semi-invariant averages. However, because of the Feynman-diagram nature of the present work, renormalization of the propagators and vertices is greatly simplified, in comparison with analysis due to Stinchcombe *et al.*, although their treatment is closely followed.

In Sec. 2, a high-density classification in powers of $1/Z$ is introduced, for the high-temperature region (above the critical point T_c) where Z is the number of spins interacting with any given spin. The $O(1)$ results are those of the well-known molecular-field theory, rigorous in the limit as Z goes to infinity. In Sec. 3, the lowest-order corrections to the two-particle propagators are of $O(1/Z)$ and give simple corrections to the transverse and longitudinal spin correlations. A low-temperature ordering is then introduced in Sec. 4 for the case $S=\frac{1}{2}$ (for simplicity), which extends the previous results to this region, where the transverse spin correlation takes on the form of simple spin-wave theory in a Green's-function (boson) formulation. The use of equivalent vertices in this section facilitates comparison with earlier spin-wave treatments, and the two lowest-order self-energy scattering graphs (evaluated in the low-temperature approximation) give the famous T^4 correction to the free energy in the first Born approximation. The corresponding graphs give the equivalent results for spin-wave renormalization, while the next graph introduces the spin-wave damping term. In both cases, explicit approximations are made which exhibit the limitations of such results.

[15] C. W. Haas and H. S. Jarrett, Phys. Rev. **135,** A1089 (1964).
[16] F. Englert, Phys. Rev. **129,** 567 (1963).
[17] R. Brout, Phys. Rev. **122,** 469 (1961).
[18] R. B. Stinchcombe, G. Horwitz, F. Englert, and R. Brout, Phys. Rev. **130,** 155 (1963).
[19] W. Lewis and R. B. Stinchcombe (unpublished).

2. MOLECULAR-FIELD THEORY

In this section the Heisenberg Hamiltonian will be transformed by means of the drone-fermion representation to a form convenient for a diagrammatic analysis of its structure. This will initially be done in terms of the representation for $S=\frac{1}{2}$, and the analogous result for $S=1$ will just be written down. A simple high-density classification of the resulting diagrams is presented, valid for temperatures above the Curie temperature T_c; this follows the analogous arguments of Stinchcombe *et al.* The simplest form of renormalization of the lowest-order self-energy in the evaluation of the magnetization $\langle S^z\rangle$ (which is also consistent with this classification) results in the Weiss molecular-field model. We shall see later that these results are also valid in the low-temperature region and include the Ising model,[16] which only involves the longitudinal component of the Heisenberg model used in this result. The well-known model of the Heisenberg ferromagnet for N equal spins, each localized on lattice sites $\mathbf{R}_i$, in the presence of an external field (giving a Zeeman splitting ω_0) is

$$H=\omega_0\sum_i S_i{}^z-\tfrac{1}{2}\sum_{i,j} I(\mathbf{R}_i-\mathbf{R}_j)\,\mathbf{S}_i\cdot\mathbf{S}_j. \qquad (2.1)$$

Since the interaction integral is only nonzero between different sites, the two sums over lattice points are complete. Moreover, because of translational symmetry, we can introduce its spatial Fourier transform

$$J(\mathbf{k})=\sum_j I(\mathbf{R}_i-\mathbf{R}_j)\,\exp[i\mathbf{k}(\mathbf{R}_i-\mathbf{R}_j)], \qquad (2.2)$$

so the above restriction on I becomes

$$\sum_{\mathbf{k}} J(\mathbf{k})=0, \qquad (2.3)$$

where the sum is over all momenta $\mathbf{k}$ in the first Brillouin zone. Substituting in Eq. (2.1) for the spin operators[4] ($S=\frac{1}{2}$), i.e.,

$$S_j{}^z=c_j{}^\dagger c_j-\tfrac{1}{2}, \qquad S_j{}^+=c_j{}^\dagger\varphi_j, \qquad (2.4)$$

using the notation of the previous paper, referred to as I, we obtain

$$H=-\tfrac{1}{2}N[\omega_0+\tfrac{1}{4}J(\mathbf{0})]+[\omega_0+\tfrac{1}{2}J(\mathbf{0})]\sum_i c_i{}^\dagger c_i$$
$$-\tfrac{1}{2}\sum_{ij} I(\mathbf{R}_i-\mathbf{R}_j)\,(c_i{}^\dagger c_i c_j{}^\dagger c_j+c_i{}^\dagger c_j\varphi_i\varphi_j). \qquad (2.5)$$

Introducing the Fourier transforms of these new operators by

$$c_i{}^\dagger=(N)^{-1/2}\sum_{\mathbf{k}}\exp(i\mathbf{k}\cdot\mathbf{R}_i)\,c_{\mathbf{k}}{}^\dagger,$$
$$\varphi_i=(N)^{-1/2}\sum_{\mathbf{k}}\exp(i\mathbf{k}\cdot\mathbf{R}_i)\,\varphi_{\mathbf{k}},$$

because of the real nature of φ_i, we have $\varphi_{\mathbf{k}}{}^\dagger=\varphi_{-\mathbf{k}}$. The complete result of these substitutions and transforma-

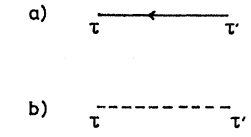

FIG. 1. Diagrammatic representation of the free "field" propagators (the drone fermions), involving temperature variables; (a) the C propagator $C^0(\tau-\tau')$, (b) the D propagator $D^0(\tau-\tau')$.

tions can be written in a separable form:

$$H=H_0+H_1. \tag{2.6}$$

The unperturbed Hamiltonian is diagonalized with respect to all the C momentum operators (we also drop the constant term because it gives no net effect)

$$H_0=B\sum_{\mathbf{k}} c_{\mathbf{k}}{}^{\dagger}c_{\mathbf{k}},$$

with

$$B=\omega_0+\tfrac{1}{2}J(\mathbf{0}). \tag{2.7}$$

The interaction term, which conserves momenta, can be further separated into a transverse part $H_1{}^T$ and a longitudinal part (or Ising term) $H_1{}^L$.:

$$H_1{}^T=-(1/2N)\sum J(\mathbf{k}+\mathbf{q})c_{\mathbf{k}}{}^{\dagger}c_{\mathbf{k}'}\varphi_{\mathbf{q}}\varphi_{-\mathbf{q}}{}'\delta(\mathbf{k}-\mathbf{k}'+\mathbf{q}-\mathbf{q}'),$$
$$H_1{}^L=-(1/2N)\sum J(\mathbf{k}-\mathbf{k}')c_{\mathbf{k}}{}^{\dagger}c_{\mathbf{k}'}c_{\mathbf{q}}{}^{\dagger}c_{\mathbf{q}'}\delta(\mathbf{k}-\mathbf{k}'+\mathbf{q}-\mathbf{q}'). \tag{2.8}$$

The sum in each case is over all four momenta variables. In terms of the interaction picture for these operators we have

$$c_{\mathbf{k}}{}^{\dagger}(\tau)=\exp(H_0\tau)c_{\mathbf{k}}{}^{\dagger}\exp(-H_0\tau)=e^{B\tau}c_{\mathbf{k}}{}^{\dagger},$$
$$\varphi_{\mathbf{q}}(\tau)=\varphi_{\mathbf{q}}. \tag{2.9}$$

The latter result implies that the temperature label τ is only used to order the φ operators. Thus the thermal averages for the unperturbed Hamiltonian become

$$\langle c_{\mathbf{k}}{}^{\dagger}c_{\mathbf{k}'}\rangle_0=\delta_{\mathbf{k}\mathbf{k}'}(e^{\beta B}+1)^{-1}=\delta_{\mathbf{k}\mathbf{k}'}f^-=\delta_{\mathbf{k}\mathbf{k}'}(1-f^+), \tag{2.10}$$

where f^- is the usual Fermi function, as in (I.12). This enables a free propagator for the C field to be defined as $C(\bar{\tau})$, with $\bar{\tau}=\tau-\tau'$:

$$C_{\mathbf{k}}{}^o(\bar{\tau})=\langle T_w(c_{\mathbf{k}}(\tau)c_{\mathbf{k}'}{}^{\dagger}(\tau'))\rangle_0$$
$$=\delta_{\mathbf{k}\mathbf{k}'}\exp(-B\bar{\tau})\ (\Theta(\bar{\tau})f^+-\Theta(-\bar{\tau})f^-); \tag{2.11}$$

similarly,

$$D_{\mathbf{q}}{}^o(\bar{\tau})=\langle T_w(\varphi_{\mathbf{q}}(\tau)\varphi_{-\mathbf{q}'}(\tau'))\rangle_0=\delta_{\mathbf{q}\mathbf{q}'}\epsilon(\bar{\tau}). \tag{2.12}$$

The effect of the temperature Wick-ordering operator is illustrated in Eq. (2.11), and $\epsilon(\tau)=\Theta(\tau)-\Theta(-\tau)$, where $\Theta(\tau)$, is the usual Heaviside-unit step function. The periodic nature of these functions with respect to $\bar{\tau}$ enables their (odd) Fourier series transforms to be written down immediately:

$$C_{\mathbf{k}}{}^o(\tau)=(1/\beta)\sum_{\bar{\nu}}{}'\exp(-i\bar{\nu}\tau)\ C_{\mathbf{k}}{}^o(\bar{\nu}),$$

with

$$C_{\mathbf{k}}{}^o(\bar{\nu})=1/(B-i\bar{\nu}), \tag{2.13}$$
$$D_{\mathbf{q}}{}^o(\tau)=(1/\beta)\sum_{\bar{\nu}}\exp(-i\bar{\nu}\tau)\ D_{\mathbf{q}}{}^o(\bar{\nu}),$$

with

$$D_{\mathbf{q}}{}^o(\bar{\nu})=-2/i\bar{\nu}. \tag{2.14}$$

The variables are defined by $\bar{\nu}=(2\nu+1)(\pi/\beta)$, and the sum is taken over all (positive and negative) integer values of ν. These functions will eventually be analytically continued into the whole of the complex ω plane with $\omega=i\bar{\nu}$. The exact propagators (in the Heisenberg picture) are related to the averages in the interaction picture by the Dyson development operator[1]

$$U(\beta)=T\exp\left(-\int_0^{\beta}d\tau_1 H_1(\tau_1)\right).$$

As we have established a Wick theorem[4] for the drone-fermion operators, we can invoke the standard proof of the linked-cluster theorem,[1] giving, for example (with superscript Ld for restriction to unique linked diagrams),

$$C_{\mathbf{k}}(\bar{\tau})=\langle T_w(c_{\mathbf{k}}(\tau)c_{\mathbf{k}}{}^{\dagger}(\tau'))\rangle$$
$$=\langle T_w(c_{\mathbf{k}}(\tau)U(\beta)c_{\mathbf{k}}{}^{\dagger}(\tau'))\rangle_0{}^{\mathrm{Ld}}.$$

The propagators are illustrated in Fig. 1; the directed solid line represents the propagator $C^o(\tau)$, while the dotted line represents a D field propagator $D_{\mathbf{q}}{}^o(\tau)$. (In the case of $S=1$, they will involve an additional index α.) The interaction can be represented by the two types of vertex, as illustrated in Fig. 2. The first vertex represents a spin-flip transition, while the second corresponds to Ising scattering.

We are now in a position to evaluate the thermal average of any product of operators, i.e., m-particle Green's functions, through the following correspondence rules between linked diagrams and their algebraic expressions:

(a) Associate propagators with their corresponding lines, and a factor $(1/2N)J(\mathbf{k}-\mathbf{k}')\delta(\mathbf{k}-\mathbf{k}'+\mathbf{q}-\mathbf{q}')$

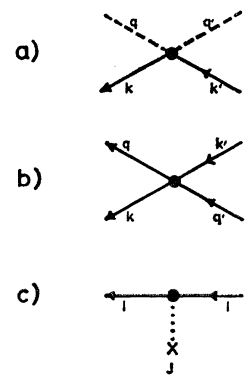

FIG. 2. The simplest interaction vertices for the Heisenberg model ($S=\frac{1}{2}$): (a) the transverse scattering or C-D scattering, (b) the longitudinal (Ising) scattering or C-C scattering, (c) extra vertex, to prevent overcounting for $S=1$.

with each longitudinal vertex and a factor

$$(1/2N)J(\mathbf{k}+\mathbf{q})\delta(\mathbf{k}-\mathbf{k}'+\mathbf{q}-\mathbf{q}')$$

with each transverse vertex.

(b) A factor $(-1)^l/r2^p$ for each diagram, where r is the symmetry factor for that structure (this prevents overcounting), p is the number of pairs of equivalent lines between vertices, and l is the number of closed loops (excepting C field self-energy loops on the same vertex).

(c) Finally, a complete summation is carried out over all internal variables and integration over all τ_i from O to β.

The high-density classification[18] arises from the observation that each vertex has a factor $J(\mathbf{k})$ (or I_{ij} upon transforming) and a label τ_i, which is eventually integrated from O to β, so we approximate its contribution by $\beta\bar{I}$, where $\bar{I}$ is some average value of $J(\mathbf{k})$. Now only the $\mathbf{k}$ dependence arising from the $J(k)$ factors as in Eq. (2.2) is important since all C^o and D^o propagators are actually independent of their momentum labels. Subsequent summation over $\mathbf{k}$ introduces a Kronecker δ reduction in the site summation

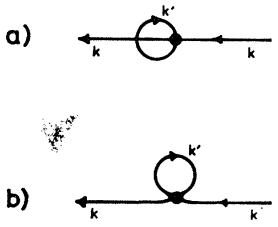

FIG. 3. The simplest C-field self-energy diagrams: (a) the direct excitation; (b) the exchange excitation.

(i or j), so a diagram involving V vertices, L of which appear with explicit $\mathbf{k}$ dependence, will give V-L independent site summations on Fourier transforming. This produces a numerical factor of order $(\beta\bar{I})^V Z^{V-L}$, where Z is the number of spins interacting with any other. But from molecular-field theory (as we shall see) the critical temperature is given by $\frac{1}{4}\beta_c J(\mathbf{0})=1$, or approximately $Z\bar{I}=kT_c$; so such a diagram will then contribute a factor $(T_c/T)^V Z^{-L}$. Thus, for temperatures above T_c, the order of the graph in the high-density expansion is Z^{-L}. In general, there will be several explicit $\mathbf{k}$ factors due to momentum conservation, so we obtain an expansion in inverse powers of Z.

The lowest-order self-energy correction to the magnetization is illustrated in Fig. 3(a). This gives for the magnetic (C field) self-energy $\Sigma_{\mathbf{k}}^{(1)}(\tau)$ a total contribution

$$\Sigma_{\mathbf{k}}^{(1)}(\tau)=J(\mathbf{0})f^{-}\delta(\tau)$$

or

$$\Sigma_{\mathbf{k}}^{(1)}(\bar{\nu})=J(\mathbf{0})f^{-}. \tag{2.15}$$

Note that the exchange term in Fig. 3(b) gives a zero contribution using Eq. (2.3). Using Dyson's equation[1]

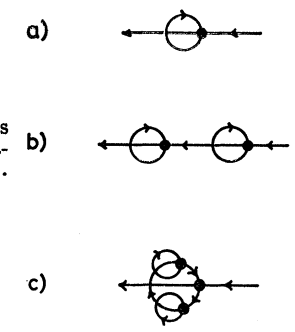

FIG. 4. Higher-order graphs involved in C-field renormalization, which are all of $O(1)$.

for the first-order propagator,

$$C_{\mathbf{k}}^{(1)}(\bar{\nu})=C_{\mathbf{k}}^{o}(\bar{\nu})+C_{\mathbf{k}}^{o}(\bar{\nu})\Sigma_{\mathbf{k}}^{(1)}(\bar{\nu})C_{\mathbf{k}}^{(1)}(\bar{\nu}), \tag{2.16}$$

we include all reducible terms of the type illustrated in Figs. 4(a) and 4(b). Both of these involve no explicit $\mathbf{k}$ dependence in the vertex factors $J(0)$, i.e., $L=0$, so that all these graphs give a contribution $O(1)$ in inverse powers of Z. However, so do all "cactus" graphs of the type illustrated in Fig. 4(c), so these too must be included. This is quite trivial and involves only converting C lines in the self-energy from free averages to full self-consistent ones. This is shown in diagrammatic form in Fig. 5, i.e.,

$$\Sigma_{\mathbf{k}}^{(1)}(C^0)\rightarrow\Sigma_{\mathbf{k}}^{1}(C^1),$$

so that

$$\Sigma_{\mathbf{k}}^{1}(\bar{\nu})=J(\mathbf{0})\langle c_{\mathbf{k}}^{\dagger}c_{\mathbf{k}}\rangle_1=J(\mathbf{0})\left(\tfrac{1}{2}+\langle S^z\rangle_1\right). \tag{2.17}$$

Thus

$$C_{\mathbf{k}}^{1}(\bar{\nu})=(B-i\bar{\nu}-\Sigma_{\mathbf{k}}^{1}(\bar{\nu}))^{-1}=[\omega_0-J(\mathbf{0})\langle S^z\rangle_1-i\bar{\nu}]^{-1}. \tag{2.18}$$

This just introduces a real shift proportional to the net magnetization. In terms of its analytic continuation to above and below the real ω axis (i.e., $i\bar{\nu}\rightarrow\omega\pm is$),

$$\begin{aligned}\mathrm{disc}C_{\mathbf{k}}^{1}(\omega)&=C_{\mathbf{k}}^{1}(\omega+is)-C_{\mathbf{k}}^{1}(\omega-is)\\&=2\pi i\delta[\omega_0-R_1J(\mathbf{0})-\omega],\end{aligned} \tag{2.19}$$

where

$$R_1=\langle S_i^z\rangle_1=\langle S_{\mathbf{k}}^z\rangle_1,$$

so that

$$C_{\mathbf{k}}^{1}(\tau)=\epsilon(\tau)(2\pi i)^{-1}\int_{-\infty}^{\infty}\frac{d\omega e^{-\omega\tau}}{1+\exp[-\beta\omega\epsilon(\tau)]}\,\mathrm{disc}C_{\mathbf{k}}^{1}(\omega), \tag{2.20}$$

where we have converted the Fermi contour from

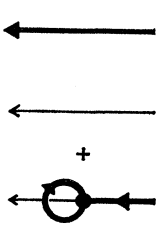

FIG. 5. The Dyson equation for molecular-field renormalization of the C propagator.

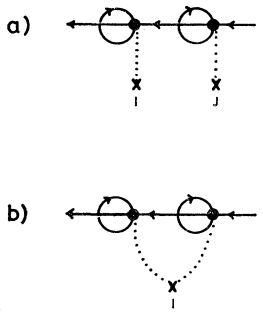

FIG. 6. Two second-order diagrams illustrating the counting correction procedure for on-site coincidences: (a) independent sites, (b) correction diagram for $i=j$.

around the imaginary ω axis (except the origin), to surround the pole on the real ω axis. This results in just replaclng B in Eq. (2.11) by $\omega_0-R_1J(\mathbf{0})$. In the limit $\tau\to 0^+$, along with Eq. (2.4), we obtain

$$R_1=-\tfrac{1}{2}\tanh\tfrac{1}{2}\beta[\omega_0-J(\mathbf{0})R_1]. \tag{2.21}$$

This is the usual molecular-field result for $S=\frac{1}{2}$ and only has a nonvanishing self-consistent result in zero field $\omega_0\to 0$ for temperatures below T_c, where $4T_c=J(\mathbf{0})$, so at low temperatures $R_1\to-\frac{1}{2}\,\mathrm{sgn}(\omega_0)$. Since this result is correct to $O(1)$, we can always renormalize all future results involving C lines by changing B to $[\omega_0-J(\mathbf{0})R_1]$ in its Fourier transform. This treatment can be seen to be the dual of the method of semi-invariants used by Stinchcombe *et al.*

The corresponding result for $S=1$ is more difficult to obtain because of the overcounting factor Y ($\frac{4}{3}\geq Y\geq 1$). This necessitates the retention of the site indices, as one must handle site coincidences very carefully. The result is to introduce additional diagrams to correct for such coincidences. The C-space substitution is now only carried out after the expansion of the Dyson development operator $U(\beta)$ in terms of sums of products of the *original* spin operators. The average of each product of these spin operators with m different site labels may be calculated as Y^m times the corresponding C-space average. The interaction part of the Hamiltonian can be written as

$$H_1=H_1^0+H_1^T+H_1^L, \tag{2.22}$$

with

$$H_1^0=\tfrac{1}{2}\sum_{i,j,\lambda,\lambda'} I(\mathbf{R}_i-\mathbf{R}_j)c_{i\lambda}{}^\dagger c_{i\lambda} \tag{2.23}$$

and

$$H_1^T=-\tfrac{1}{2}\sum_{ij\lambda\lambda'} I(\mathbf{R}_i-\mathbf{R}_j)c_{i\lambda}{}^\dagger\phi_{i\lambda}\phi_{j\lambda'}c_{j\lambda'}, \tag{2.24}$$

$$H_1^L=-\tfrac{1}{2}\sum_{ij\lambda\lambda'} I(\mathbf{R}_i-\mathbf{R}_j)c_{i\lambda}{}^\dagger c_{i\lambda}c_{j\lambda'}{}^\dagger c_{j\lambda'}, \tag{2.25}$$

where the two 'spin indices' λ, $\lambda'=1, 2$.

The term H_1^0 cannot be incorporated with the H_0 term as in Eq. (2.7), as it involves two site summations, not just one. It is represented diagrammatically in Fig. 2(c), where the labelled cross indicates the second site index. Now in any of the graphs with L-site summations there will be terms corresponding to coincidences on some of the sites, and these will give a lower power in the counting factor Y. As usual, these are represented by diagrams with c dotted lines converging at the same cross. However, these correction diagrams are always $O(Z^{-c})$, relative to the same diagrams with independent summations. For example, the second-order diagram in Fig. 6 illustrates an $O(J^2)$ term, including the correction diagram Fig. 6(b). The diagram 6(a) gives a factor $[YJ(0)]^2$, while the correction term 6(b) leads to a factor $(Y-Y^2)\sum_i I^2(\mathbf{R}_i-\mathbf{R}_j)$. In calculating the magnetization to $O(Z^0)$ all these correction terms can be neglected. The self-energy is then

$$\Sigma_{ij}{}^{\lambda\lambda'}(\tau)=\delta_{\lambda\lambda'}\delta_{ij}\delta(\tau)\,Y\sum_{l,\gamma} I\,(\mathbf{R}_i-\mathbf{R}_l)\{\langle c_{l\gamma}{}^\dagger c_{l\gamma}\rangle_0{}^c-\tfrac{1}{2}\} \tag{2.26}$$

or, in a reduced notation, using Eq. (1.17),

$$\Sigma_{i\lambda}{}^{(1)}(\bar{\nu})=Y(2f^-\!-1)J(\mathbf{0})=J(\mathbf{0})\langle S^z\rangle_0{}^s. \tag{2.27}$$

Note that the counting factor is just sufficient to introduce the spin-averaged magnetization $R_s{}^0$ and not the C-space average $R_c{}^0$. The $O(1)$ magnetization is then

$$R_s{}^{(1)}=-Y\tanh\tfrac{1}{2}\beta[\omega_0-R_s{}^0J(\mathbf{0})]. \tag{2.28}$$

In the same manner as for $S=\frac{1}{2}$ we can use the renormalized fermion line for the internal "molecular-field" loop with the result

$$R_s{}^1=-Y\tanh\tfrac{1}{2}\beta[\omega_0-R_s{}^1J(\mathbf{0})]. \tag{2.29}$$

Apart from the counting factor Y (of order unity), this is directly analogous to Eq. (2.22). The difficulties with this $S=1$ method occur equally in the Yolin–Abrikosov technique, even for $S=\frac{1}{2}$, which demonstrates the advantage of the present spin-$\frac{1}{2}$ method.

3. TRANSVERSE AND LONGITUDINAL CORRELATIONS AT HIGH TEMPERATURES

In this section we shall extend the calculation to the next order in the high-density classification, that is, to order $1/Z$. This will now include all diagrams with only one explicit $\mathbf{k}$ dependence, e.g., $J(\mathbf{k})^n$; accordingly, all these will have $L=1$, giving a contribution of $O(1/Z)$. Figure 7 shows that these are the simple repeated scattering graphs for the two-particle propagators, corresponding to the transverse and longitudinal

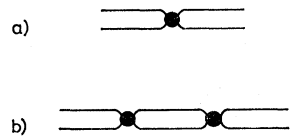

FIG. 7. Renormalization graphs for two-particle propagators, which are of $O(1/Z)$ in the high-density classification.

correlations $\langle S^-S^+\rangle$ and $\langle S^zS^z\rangle$, respectively. In the next section we shall show that this class of graphs chosen by the simple high-density classification and so strictly valid only for $T>T_c$ (as shown earlier) are also the same as those corresponding to the low-order terms in the expansion in powers of the temperature, so the present results will also be valid in the whole temperature regime (apart from the critical region), and the transverse correlations will reduce to the results of low-temperature spin-wave theory.

The case for $S=\frac{1}{2}$ will again be taken, for simplicity, and the generalization for $S=1$ indicated. We will define a spin-wave propagator $F(\mathbf{k},\tau)$ in terms of the Fourier transforms of the transverse correlation functions. Let

$$\mathbf{S}_i=(N)^{-1/2}\sum_{\mathrm{k}}\exp(i\mathbf{k}\cdot\mathbf{R}_i)\,\mathbf{S}_{\mathrm{k}},$$

then

$$(S^+)_{\mathrm{k}}=(N)^{-1/2}\sum_{\mathbf{q}}c_{\mathrm{k+q}}{}^{\dagger}\varphi_{-\mathrm{q}}, \tag{3.1}$$

so that

$$F(\mathbf{k},\tau)=\langle T[S_{-\mathrm{k}}{}^-(\tau)\,S_{\mathrm{k}}{}^+(0)]\rangle. \tag{3.2}$$

This even periodic function will be analyzed in terms of its components

$$F(\mathbf{k},\tau)=(1/N)\sum_{\mathrm{qq'}}F_{\mathrm{qq'}}(\mathbf{k},\tau), \tag{3.3}$$

where

$$F_{\mathrm{qq'}}(\mathbf{k},\tau)=\langle T_w(\varphi_{\mathrm{q}}(\tau^+)c_{\mathrm{k+q}}(\tau)c_{\mathrm{k+q'}}{}^{\dagger}(0^+)\varphi_{-\mathrm{q'}}(0))\rangle. \tag{3.4}$$

The zeroth-order form of this propagator has the simple structure

$$F_{\mathrm{qq'}}{}^0(\mathbf{k},\tau)=\delta_{\mathrm{qq'}}D_{\mathrm{q}}{}^0(\tau)C_{\mathrm{k+q}}{}^0(\tau)$$
$$=\delta_{\mathrm{qq'}}e^{-B\tau}[\Theta(\tau)f^+ +\Theta(-\tau)f^-]. \tag{3.5}$$

This is illustrated in Fig. 8, and its (even) Fourier transform is given by [with $\bar{\alpha}=(2\pi/\beta)\alpha$, α are all integers]

$$F_{\mathrm{q}}{}^0(\mathbf{k},\tau)=(\beta)^{-1}\sum_{\alpha}\exp(-i\bar{\alpha}\tau)\;F_{\mathrm{q}}{}^0(\mathbf{k},\bar{\alpha}),$$

$$F_{\mathrm{q}}{}^0(\mathbf{k},\bar{\alpha})=\tanh\tfrac{1}{2}\beta B/(B-i\bar{\alpha}). \tag{3.6}$$

The $1/Z$ series is generated from the lowest-order self-energy of this propagator, $\Xi_{\mathrm{qq'}}(\mathbf{k},\tau)$, which is illustrated in Fig. 9 and defined by a general correction to $F_{\mathrm{qq'}}(\mathbf{k},\tau)$:

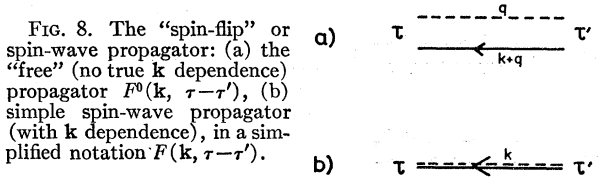

FIG. 8. The "spin-flip" or spin-wave propagator: (a) the "free" (no true k dependence) propagator $F^0(\mathbf{k},\tau-\tau')$, (b) simple spin-wave propagator (with k dependence), in a simplified notation $F(\mathbf{k},\tau-\tau')$.

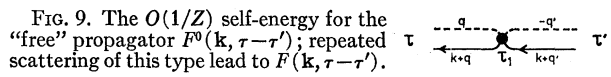

FIG. 9. The $O(1/Z)$ self-energy for the "free" propagator $F^0(\mathbf{k},\tau-\tau')$; repeated scattering of this type lead to $F(\mathbf{k},\tau-\tau')$.

$$F_{\mathrm{qq'}}(\mathbf{k},\tau)$$
$$=\int_0^{\beta}\!\!\int d\tau_1 d\tau_2 F_{\mathrm{q}}{}^0(\mathbf{k},\tau-\tau_1)\,\Xi_{\mathrm{qq'}}(\mathbf{k},\tau_1-\tau_2)\,F_{\mathrm{q'}}{}^0(\mathbf{k},\tau_2). \tag{3.7}$$

Upon evaluation this gives

$$\Xi_{\mathrm{qq'}}{}^{(1)}(\mathbf{k},\tau)=(1/2N)J(\mathbf{k})\delta(\tau),$$
$$\Xi_{\mathrm{qq'}}{}^{(1)}(\mathbf{k},\bar{\alpha})=(1/2N)J(\mathbf{k}). \tag{3.8}$$

The appropriate Dyson equation for this series (including the free summations in the intermediate states) is

$$F_{\mathrm{qq'}}{}^{(1)}(\mathbf{k},\bar{\alpha})=F_{\mathrm{qq'}}{}^0(\mathbf{k},\bar{\alpha})$$
$$+\sum_{\mathrm{q''}}F_{\mathrm{q}}{}^0(\mathbf{k},\bar{\alpha})\,\Xi_{\mathrm{qq''}}{}^{(1)}(\mathbf{k},\bar{\alpha})\,F_{\mathrm{q''},\mathrm{q'}}{}^{(1)}(\mathbf{k},\bar{\alpha}) \tag{3.9}$$

or

$$F^{(1)}(\mathbf{k},\bar{\alpha})=(1/N)\sum_{\mathrm{qq'}}F_{\mathrm{qq'}}{}^{(1)}(\mathbf{k},\bar{\alpha})$$
$$=([F^0(\mathbf{k},\bar{\alpha})]^{-1}-N\Xi^{(1)}(\mathbf{k},\bar{\alpha}))^{-1}. \tag{3.10}$$

Substituting for $F^0(\mathbf{k},\bar{\alpha})$ and $\Xi^{(1)}(\mathbf{k},\bar{\alpha})$ by Eqs. (3.6) and (3.8),

$$F^{(1)}(\mathbf{k},\bar{\alpha})=\frac{\tanh\frac{1}{2}\beta B}{\omega_0+\frac{1}{2}[J(0)-J(\mathbf{k})\tanh\frac{1}{2}\beta B]-i\bar{\alpha}}. \tag{3.11}$$

However, first-order renormalization of the constituent C propagators will not change the order of $1/Z$ of these graphs, so by Eq. (2.21) the molecular-field transverse propagator becomes

$$F_{\mathrm{qq'}}{}^0(\mathbf{k},\bar{\alpha})=-\delta_{\mathrm{qq'}}2R^1/[\omega_0-R^1J(0)-i\bar{\alpha}]. \tag{3.12}$$

Upon including the transverse self-energy, we finally obtain

$$F^1(\mathbf{k},\bar{\alpha})=-2R^1\{\omega(\mathbf{k})-i\bar{\alpha}\}^{-1}, \tag{3.13}$$

where

$$\omega(\mathbf{k})=\omega_0-R^1\{J(0)-J(\mathbf{k})\}. \tag{3.14}$$

The appropriate correlation functions can be calculated immediately by converting the $\bar{\alpha}$ summation to the 'Bose contour,' which encircles the whole of the imaginary z axis in an anticlockwise direction, with $z=i\bar{\alpha}$. This results in

$$F^1(\mathbf{k},\tau)=\frac{-\epsilon(\tau)2R^1\exp\{-\omega(\mathbf{k})\tau\}}{1-\exp\{-\beta\omega(\mathbf{k})\epsilon(\tau)\}}. \tag{3.15}$$

So the lowest-order $[O(1/Z)]$ transverse interaction effects a k-dependent energy shift with no damping.

The analogous result for $S=1$ cannot be so simply obtained because of the resulting complexity arising from the counting factor. An equation similar to Eq. (3.9) can be written down in terms of the following propagator and in the site-index representation:

$$F_{ij,\lambda\lambda'}(\tau)=\langle T\{\phi_{i\lambda}(\tau^+)c_{i\lambda}(\tau)c_{j\lambda'}{}^\dagger(0^+)\phi_{j\lambda'}(0)\}\rangle^c, \quad (3.16)$$

with

$$\Xi_{ij,\lambda\lambda'}(\bar{\alpha})=\tfrac{1}{2}I(\mathbf{R}_i-\mathbf{R}_j).$$

This equation can be formally solved in terms of the momentum Fourier components, but this introduces compensation complications which destroy the elegance of the $S=\frac{1}{2}$ result. In other words, the correspondence between the spin-space and C-space transverse propagators depends on whether or not the site indices are equal:

$$\langle T\{S_i^-(\tau)S_j^+(0)\}\rangle_0{}^s=\{Y+\delta_{ij}(Y^2-Y)\}F_{ij,\lambda\lambda'}{}^0(\tau). \quad (3.17)$$

The other series of graphs which are also of order $1/Z$ are the longitudinal graphs, Fig. 7. However, in this case, because of the identity of the four operators, a nonpropagated part must first be subtracted. Thus for $\langle S_i{}^zS_j{}^z\rangle$ we have

$$\langle S_i{}^zS_j{}^z\rangle=\langle c_i{}^\dagger c_ic_j{}^\dagger c_j\rangle-\tfrac{1}{2}\langle S_i{}^z\rangle-\tfrac{1}{2}\langle S_j{}^z\rangle-\tfrac{1}{4}. \quad (3.18)$$

We consider the two-particle propagator $K_{ij}(\tau)$ and its triple Fourier transform (assuming an homogeneous system) $K_{\mathbf{qq}'}(\mathbf{k},\tau)$, defined by

$$K_{ij}(\tau)=\langle T\{c_i{}^\dagger(\tau^+)c_i(\tau)c_j{}^\dagger(0^+)c_j(0)\}\rangle^c$$
$$=N^{-1}\sum_{\mathbf{kqq}'}\exp[i\mathbf{k}\cdot(\mathbf{R}_i-\mathbf{R}_j)]K_{\mathbf{qq}'}(\mathbf{k},\tau). \quad (3.19)$$

Then

$$K_{\mathbf{qq}'}(\mathbf{k},\tau)=\langle T\{c_{\mathbf{k}+\mathbf{q}}{}^\dagger(\tau^+)c_{\mathbf{q}}(\tau)c_{\mathbf{q}'-\mathbf{k}}{}^\dagger(0^+)c_{\mathbf{q}'}(0)\}\rangle^c. \quad (3.20)$$

This can always be decomposed into two parts—a self-interaction and a propagated term $\tilde{K}$:

$$K_{\mathbf{qq}'}(\mathbf{k},\tau)=\tilde{K}_{\mathbf{qq}'}(\mathbf{k},\tau)+\delta_{\mathbf{k},0}\langle c_{\mathbf{q}}{}^\dagger c_{\mathbf{q}}\rangle\langle c_{\mathbf{q}'}{}^\dagger c_{\mathbf{q}'}\rangle. \quad (3.21)$$

This separation is just sufficient to give the usual form for the longitudinal correlation:

$$\langle S_i{}^zS_j{}^z\rangle-\langle S_i{}^z\rangle\langle S_j{}^z\rangle$$
$$=N^{-1}\sum_{\mathbf{kqq}'}\exp[i\mathbf{k}\cdot(\mathbf{R}_i-\mathbf{R}_j)]\tilde{K}_{\mathbf{qq}'}(\mathbf{k},0^+). \quad (3.22)$$

The lowest-order component graph of the propagated type is the simple particle-hole pair of noninteracting C fields. This is illustrated in Fig. 10(a), and is given by the simplest contractions:

$$\tilde{K}_{\mathbf{qq}'}{}^0(\mathbf{k},\tau)=-\delta_{\mathbf{q}',\mathbf{k}+\mathbf{q}}C_{\mathbf{q}}{}^0(\tau)C_{\mathbf{k}+\mathbf{q}}{}^0(-\tau)=\delta_{\mathbf{q}',\mathbf{k}+\mathbf{q}}f^+f^-. \quad (3.23)$$

The self-energy terms $O(1/Z)$ in the high-density expansion are illustrated in Figs. 10(b) and 10(c). Explicit evaluation of the 'exchange' graph, Fig. 10(c), demonstrates that it gives no net contribution, as it involves a self-contained interaction sum Eq. (2.3). However, the 'direct' graph Fig. 10(b) gives a nonvanishing self-energy contribution

$$A_{\mathbf{pp}'}(\mathbf{k})=(1/N)\beta J(\mathbf{k}).$$

This series is summed by using the Dyson equation

$$\tilde{K}_{\mathbf{qq}'}(\mathbf{k})=\tilde{K}_{\mathbf{qq}'}{}^0(\mathbf{k})+\sum_{\mathbf{pp}'}\tilde{K}_{\mathbf{qp}}{}^0(\mathbf{k})A_{\mathbf{pp}'}(\mathbf{k})\tilde{K}_{\mathbf{p}'\mathbf{q}'}(\mathbf{k}). \quad (3.24)$$

The temperature variables τ have been dropped in this equation, as each component of the equation (to this order) has no explicit τ dependence; we obtain immediately an algebraic equation. Summing over the indices $\mathbf{q}$ and $\mathbf{q}'$ and substituting Eq. (3.23) for $\tilde{K}_{\mathbf{qq}'}{}^0(\mathbf{k})$ leads to the final result

$$\langle S_i{}^zS_j{}^z\rangle-\langle S_i{}^z\rangle\langle S_j{}^z\rangle=N^{-1}\sum_{\mathbf{k}}\frac{\exp[i\mathbf{k}\cdot(\mathbf{R}_i-\mathbf{R}_j)]f^+f^-}{[1-\beta J(\mathbf{k})f^+f^-]}. \quad (3.25)$$

Thus, the complete $O(1/Z)$ result is obtained by renormalizing the individual C propagators. This is equivalent to the substitution $f^\pm\rightarrow\frac{1}{2}\mp R_i$, giving[18]

$$\langle S_i{}^zS_j{}^z\rangle-\langle S_i{}^z\rangle\langle S_j{}^z\rangle$$
$$=N^{-1}\sum_{\mathbf{k}}\frac{\exp[i\mathbf{k}\cdot(\mathbf{R}_i-\mathbf{R}_j)](\frac{1}{4}-R_1{}^2)}{1-\beta J(\mathbf{k})(\frac{1}{4}-R_1{}^2)}. \quad (3.26)$$

4. LOW-TEMPERATURE EXPANSION AND SPIN-WAVE SCATTERING

At this stage we shall extend the calculations to low temperatures for $S=\frac{1}{2}$, and extend the validity of the above results to temperatures below T_c, as well as recovering the low-temperature spin-wave results found by other methods. In this temperature regime the graphs can be classified by their contributions to the free-energy F in powers of the temperature (in fact, the reduced temperature T/T_c). In order to do this systematically, we must analyze the contributions of each individual type of element in the graphs. Upon summation over $\bar{\nu}$ of $C^0(\bar{\nu})$ there will result a factor

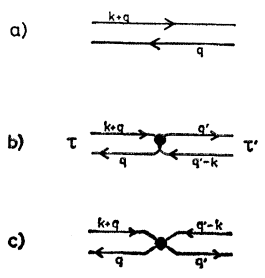

FIG. 10. The longitudinal-correlation propagator, $K_{\mathbf{qq}'}(\mathbf{k},\tau-\tau')$: (a) the free propagator, $K_{\mathbf{qq}'}{}^0(\mathbf{k},\tau-\tau')$, (b) the $O(1/Z)$ direct-scattering graph leading to $K^{(1)}(\mathbf{k},\tau)$, (c) the $O(1/Z)$ exchange-scattering graph.

f^+ or f^- which, with simple molecular-field renormalization, becomes $f^\pm \to \frac{1}{2} \mp R_1$. Then, in the two limits $T \to 0$ and $\omega_0 \to 0^+$, these become $f^+ \to 1 - \exp[-\beta J(\mathbf{0})/2]$ and $f^- \to \exp[-\beta J(\mathbf{0})/2]$, or, in the corresponding limit of $\omega_0 \to 0^-$, the roles of $f^\pm$ are reversed as $R \to -\frac{1}{2}\,\mathrm{sgn}(\omega_0)$, so at low temperatures, in zero magnetic field, with ferromagnetic interactions $J(\mathbf{0}) > 0$, the factor $\exp[-\beta J(\mathbf{0})/2]$ is negligible compared with any finite power of T. This implies that any "particle-hole" pair of C propagators occurring between any two vertices will introduce a factor f^+f^- upon integration over the internal temperature variables, so all such graphs will be exponentially small and can be neglected. D propagators always give a finite contribution of $O(1)$, as do unpaired C propagators in the correct limit. The next contributing element is the simple spin-wave (i.e., with $\mathbf{k}$ dependence introduced through one transverse vertex). Since at low temperatures Eq. (3.13) gives

$$F(\mathbf{k}, \bar{\alpha}) = [\tfrac{1}{2}(J(0) - J(\mathbf{k})) - i\bar{\alpha}]^{-1} \tag{4.1}$$

or

$$F(\mathbf{k}, \tau) = \exp[-\omega(\mathbf{k})\tau][\Theta(\tau) b_{\mathbf{k}}^+ + \Theta(-\tau) b_{\mathbf{k}}^-], \tag{4.2}$$

with

$$\omega(\mathbf{k}) = \tfrac{1}{2}[J(0) - J(\mathbf{k})],$$
$$b_{\mathbf{k}}^+ = 1 + b_{\mathbf{k}}^- = (1 - \exp[-\beta\omega(\mathbf{k})])^{-1}. \tag{4.3}$$

This is represented by a simple line as in Fig. 8(b). We can now simplify all graphs by isolating all spin-wave lines which then interact via equivalent vertices V represented by Fig. 11(a); these vertices will contain only C and D substructure and correspond explicitly to the kinematical corrections in ideal spin-wave theory. As we are now dealing with a standard type of quantum-field theory, the contributions to the change in the free-energy F due to the interactions are given by the usual sum of distinct connected graphs:

$$-\beta\Delta F = \langle U(\beta) \rangle_0^{\text{con}}. \tag{4.4}$$

Again we will follow the low-temperature classification

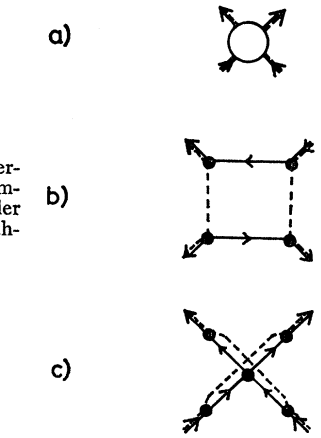

FIG. 11. The equivalent vertex, V: (a) complete diagrammatic graph, (b) 4th-order equivalent vertex, (c) 5th-order equivalent vertex.

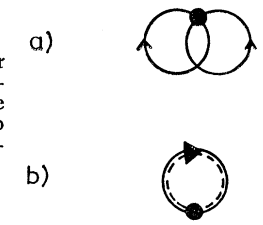

FIG. 12. The two lowest-order contributions, in the low-temperature series, to the change in the free energy ΔF: (a) the Ising loop $O(1)$, (b) the transverse (spin-wave) loop, $O(T^{3/2})$.

method used by Stinchcombe *et al.*[18] for their semi-invariant analysis and find a very close correspondence for the present Green's-function approach. The equivalent vertices only involve functions of $J(\mathbf{k})$ and poles of the form $(B - i\bar{\alpha})^{-n}$, which lead to exponentially small corrections at B, but are converted to $[\frac{1}{2}J(\mathbf{k})]^n$ at the spin-wave poles $i\bar{\alpha} = \omega(\mathbf{k})$ and so only result in one power of β per vertex as a result of equivalent energy conservation at this "vertex." Consider a graph with N spin-wave lines interacting through V equivalent vertices and resulting in S-independent $\mathbf{k}$ and $\bar{\alpha}$ summations. Each of the S sums over $\bar{\alpha}_j$ is converted into a Bose contour around the whole of the imaginary ω_j axis, where $\omega_j = i\bar{\alpha}_j$. This is then distorted in the usual manner to pick up the residues of the poles from the product of the spin-wave denominators. The net result is a product of spin-wave Bose occupation factors $b_{\mathbf{k}}^-$ multiplied by a product of $(N-S)$ denominators, each of the form $\sum_j \omega(\mathbf{k}_j)$. The contribution of such a graph to $-\beta\Delta F$ has the form (retaining only temperature-dependent factors)

$$(\beta)^{V-N+S} \sum_{\mathbf{k}i} (b_{\mathbf{k}}^-)^S (\tilde{\omega})^{S-N},$$

which is proportional to $T^{(3/2)S-V}$.

However, in all but the simplest cases, this rule needs two modifications. The first exception occurs when there are D-degenerate spin waves in the graph, i.e., with the same momentum and energy $(\mathbf{k}, \bar{\alpha})$. Then the pole from this will give a contribution obtained by differentiating $(D-1)$ times the rest of the integrand with respect to $\bar{\alpha}$, so reducing the power of $\tilde{\omega}$ in the denominator from $(N-S)$ by a further $(D-1)$. This gives a contribution to $-\beta\Delta F$ of the form

$$\beta^{(V-N+S)} \sum_{\mathbf{k}_1 \cdot \mathbf{k}_s} (b_{\mathbf{k}}^-)^S (\tilde{\omega})^{-N+S+D-1},$$

which is proportional to $T^{(3/2)S-V+D-1}$. The second case arises when the frequency of one spin wave appears with opposite sign in the frequency of another because of frequency (or energy) conservation at the vertices. Effectively, there exists particle and hole spin-wave states between some of the vertices. These two poles contribute to the sum over this frequency: one yielding $b_{\mathbf{k}}^-$, leading to the usual $T^{3/2}$ contribution; the other, $b_{\mathbf{k}}^+$, which involves no temperature-dependent cutoff, and so fails to give an $O(T^{3/2})$ contribution. However, it does still give a factor $\tilde{\omega}$ in the denominator, so for S' spin-wave holes the contribution to $-\beta\Delta F$ will be

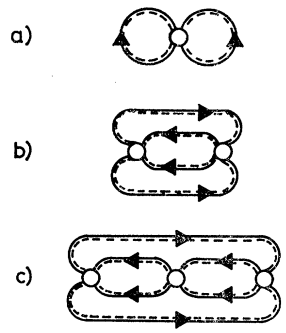

FIG. 13. The $O(T^3)$ contributions, from spin-wave scattering to the change in the free energy: (a) the first Born approximations, giving Dyson's T^4, (b) and (c) higher Born approximations, leading to damping in the spin-wave excitations.

$\beta^V(b_{\mathbf{k}'}{}^+/\beta\bar{\omega})^{S'}(b_{\mathbf{k}}{}^-)^{S-S'}(\beta\bar{\omega})^{S+S'-N}$, which is proportional to $T^{(3/2)(S-S')+S'-V}$. So, in general, a graph involving S-independent spin waves, of which S' appear both with positive and negative sign in the energies, interacting through V equivalent vertices and with N_D groups of D-degenerate resulting spin waves, will contribute to $-\beta\Delta F$ a term

$$-\beta\Delta F(S, S', V, N_D) \propto T^{[3/2(S-S')+S'-V+\Sigma_D N_D(D-1)]}. \quad (4.5)$$

Since $S>V+1$, the lowest-order graphs are those with V and N_D small. All graphs with $N_D>0$ are at least of $O(T^{7/2})$ and increase rapidly with N_D; similarly, one must minimize the number of independent spin waves. The only diagrams which give a contribution to ΔF of T^3 or less are those illustrated in Figs. 12 and 13.

Thus the two lowest-order diagrams in powers of T are also the same as those classified in powers of $1/Z$, so the results of sections (4) and (5) are also valid at low temperatures.

We shall now evaluate the low-temperature diagrams involved in spin-wave scattering to exhibit the degree of correspondence with earlier theories. This will involve calculating the effects of the vertices illustrated in Figs. 11(b) and 11(c) in the first diagram of the Born series, Fig. 13(a). Since the spin waves involve a C and D pair, then the structure of the simple interaction vertices, Fig. 2(a), indicates that the lowest-order spin-wave interactions will occur in 4th order. This vertex will be denoted by $V^{(4)}$ (the diagram obtained by interchanging the D-on pair will be included in this). If we denote the contribution of the two spin waves by $W(\mathbf{k}_1\tau_1, \mathbf{k}_2\tau_2; \mathbf{k}_3\tau_3, \mathbf{k}_4\tau_4)$, then the contribution of this graph to $-\beta\Delta F$ is given by

$$\frac{1}{(2N)^4}\sum_{\mathbf{k}i}\int_0^\beta d\tau_1, \cdots, d\tau_4 W(\mathbf{k}_1\tau_1, \cdots, \mathbf{k}_4\tau_4)\, V^{(4)}(\mathbf{k}_1\tau_1, \cdots, \mathbf{k}_4\tau_4), \quad (4.6)$$

which, on Fourier transforming with respect to the τ labels and integrating, gives (in terms of the reduced vertex $\bar{V}$)

$$[N^2/2(2N)^4]\sum_{\mathbf{k}\mathbf{k}'} J^2(\mathbf{k})J^2(\mathbf{k}')\,(1/\beta^2)\sum_{\alpha\alpha'} F(\mathbf{k}, \bar{\alpha})F(\mathbf{k}', \bar{\alpha}')\,\bar{V}^{(4)}(\bar{\alpha}\bar{\alpha}'; \bar{\alpha}'\bar{\alpha}), \quad (4.7)$$

where $\bar{V}^{(4)}(\bar{\alpha}_i)$ is the transform of $\bar{V}^{(4)}(\tau_i)$, which is given by

$$\bar{V}^{(4)}(1, 2; 3, 4) = NC^o(14)C^o(23)[D^o(12)D^o(34) - D^o(13)D^o(24)]$$
$$-NC^o(24)C^o(13)[D^o(12)D^o(34) + D^o(14)D^o(23)]. \quad (4.8)$$

The simplified notation $C^o(14) = C^o(\tau_1 - \tau_4)$ has been used here for convenience, and the factor N comes from one net internal momentum summation; the Fourier transform is given by

$$\bar{V}^{(4)}(\bar{\alpha}_1\bar{\alpha}_2; \bar{\alpha}_3\bar{\alpha}_4) = \sum_{\bar{\nu}} N\delta(1+2-3-4)C^o(\bar{\alpha}_1 - \bar{\nu})D^o(\bar{\nu})\{D^o(\bar{\alpha}_4 - \bar{\alpha}_1 + \bar{\nu})[C^o(\bar{\alpha}_2 + \bar{\nu}) - C^o(\bar{\alpha}_3 - \bar{\nu})]$$
$$+D^o(\bar{\alpha}_3 - \bar{\alpha}_1 + \bar{\nu})[C^o(\bar{\alpha}_2 + \bar{\nu}) - C^o(\bar{\alpha}_4 - \bar{\nu})]\}. \quad (4.9)$$

This is evaluated in the usual manner of converting the sum to an integral over $z = i\bar{\nu}$, involving the Fermi contour around the imaginary z axis (except for the origin). In the low-temperature approximation this only picks up the residues at the origin and those poles which result in f^+ factors (the f^- ones are exponentially small and can be neglected). Within this approximation

$$\bar{V}^{(4)}(\bar{\alpha}_1\bar{\alpha}_2; \bar{\alpha}_3\bar{\alpha}_4) = \frac{-2N\beta\delta(1+2-3-4)\,(B - i\bar{\alpha}_1 + B - i\bar{\alpha}_2)}{(B - i\bar{\alpha}_1)(B - i\bar{\alpha}_2)(B - i\bar{\alpha}_3)(B - i\bar{\alpha}_4)}. \quad (4.10)$$

Again in the low-temperature approximation the double sum over α and α' picks up the residues only at the respective spin-wave energies $\omega(\mathbf{k}_i)$, and, using $B - \omega(\mathbf{k}_i) = \frac{1}{2}J(\mathbf{k}_i) \neq 0$,

$$(1/\beta^2)\sum_{\alpha\alpha'} F(\mathbf{k}, \bar{\alpha})F(\mathbf{k}', \bar{\alpha}')\,\bar{V}^{(4)}(\bar{\alpha}\bar{\alpha}'; \bar{\alpha}'\bar{\alpha})$$
$$= -2^4\beta N b_k{}^- b_{k'}{}^-[(J(\mathbf{k}) + J(\mathbf{k}'))/J^2(\mathbf{k})J^2(\mathbf{k}')]. \quad (4.11)$$

Thus, the simple 4th-order terms result in a contribution

$$-\beta\Delta F^{(4)} = -(\beta/2N)\sum_{\mathbf{k}\mathbf{k}'} b_{\mathbf{k}}{}^- b_{\mathbf{k}'}{}^-[J(\mathbf{k}) + J(\mathbf{k}')]. \quad (4.12)$$

Similarly, for the 5th-order vertex $V^{(5)}$ we have

$$(N^3/2(2N)^4\beta^2)\sum_{\mathbf{k}\mathbf{k}'\alpha,\alpha'} J^2(\mathbf{k})J^2(\mathbf{k}') \times[J(\mathbf{k}-\mathbf{k}')+J(\mathbf{0})]F(\mathbf{k},\bar{\alpha})F(\mathbf{k}',\bar{\alpha}')\bar{V}^{(5)}(\bar{\alpha}\bar{\alpha}'\bar{\alpha}'\bar{\alpha}), \tag{4.13}$$

with

$$\bar{V}^{(5)}(\tau_i)=\int_0^\beta d\tau_5 C^o(15)C^o(25)C^o(53)C^o(54)D^o(14)D^o(23). \tag{4.14}$$

The Fourier transform of this, at low temperatures, is

$$\bar{V}^{(5)}(\bar{\alpha}_1\bar{\alpha}_2;\bar{\alpha}_3\bar{\alpha}_4)=\frac{\beta\delta(\bar{\alpha}_1+\bar{\alpha}_2-\bar{\alpha}_3-\bar{\alpha}_4)}{(B-i\bar{\alpha}_1)(B-i\bar{\alpha}_2)(B-i\bar{\alpha}_3)(B-i\bar{\alpha}_4)}, \tag{4.15}$$

so

$$(1/\beta^2)\sum_{\alpha\alpha'} F(\mathbf{k},\bar{\alpha})F(\mathbf{k}',\bar{\alpha}')\bar{V}^{(5)}(\bar{\alpha}\bar{\alpha}',\bar{\alpha}'\bar{\alpha}) = 2^4\beta b_k^- b_{k'}^-/J^2(\mathbf{k})J^2(\mathbf{k}'). \tag{4.16}$$

This gives a contribution

$$-\beta\Delta F^{(5)}=(\beta/2N)\sum_{\mathbf{k}\mathbf{k}'} b_{\mathbf{k}}^- b_{\mathbf{k}'}^-[J(\mathbf{k}-\mathbf{k}')+J(\mathbf{0})]. \tag{4.17}$$

So to $O(T^3)$ in contributions to ΔF we have

$$\Delta F^{(4+5)}=(1/2N)\sum_{\mathbf{k}\mathbf{k}'} b_{\mathbf{k}}^- b_{\mathbf{k}'}^- \times[J(\mathbf{k})+J\,\mathbf{k}')-J(\mathbf{k}-\mathbf{k}')-J(\mathbf{0})]. \tag{4.18}$$

This is the well-known result for spin-wave scattering in the first Born approximation at low temperatures obtained by Dyson,[5] who also showed the cancellation to $O(T^3)$ giving the famous $O(T^4)$ result.

If we define the sum of these two vertices as V, then we can derive all the relevant low-temperature spin-wave results directly, so

$$V(1,2;3,4)=V^{(4)}(1,2;3,4)+NV^{(5)}(1,2;3,4). \tag{4.19}$$

In the low-temperature region this has the transform

$$V(p_1p_2,p_3p_4)=\frac{\frac{1}{2}\beta N\delta(p_1+p_2-p_3-p_4)J(\mathbf{k}_1)\cdots J(\mathbf{k}_4)[J(\mathbf{k}_1-\mathbf{k}_4)-2B+i\bar{\alpha}_1+i\bar{\alpha}_2]}{(B-i\bar{\alpha}_1)(B-i\bar{\alpha}_2)(B-i\bar{\alpha}_3)(B-i\bar{\alpha}_4)}, \tag{4.20}$$

where we have used the 4-dimensional notation $p_i=\mathbf{k}_i,\bar{\alpha}_i$. We can now renormalize the simple spin waves $F(\mathbf{k},\omega)$ through the vertex V to the renormalized form $F^r(\mathbf{k},\omega)$ by means of a Dyson equation directly analogous to the one for C-propagator renormalization in the molecular-field approximation, i.e., as illustrated in Fig. 6. So upon taking into account all possible exit and entry vertex points, we obtain for the spin-wave self-energy $\Xi^r(\mathbf{k},\omega)$:

$$\Xi_{qq'}{}^r(\mathbf{k},\alpha)=[N/(2N)^4\beta^2]\sum_{\mathbf{k}'\alpha'} F(\mathbf{k}',\alpha')\,(V(\mathbf{pp}',\mathbf{pp}') +V(\mathbf{pp}',\mathbf{p}'\mathbf{p})+V(\mathbf{p}'\mathbf{p},\mathbf{p}'\mathbf{p})+(\mathbf{p}'\mathbf{p},\mathbf{pp}')), \tag{4.21}$$

which, in the low-temperature approximation, becomes

$$(2N)^{-2}[J(k)^2/(B-i\bar{\alpha})^2]\sum_{\mathbf{k}'} b_{\mathbf{k}'}^- \times[J(\mathbf{0})+J(\mathbf{k}-\mathbf{k}')-J(\mathbf{k}')-2(B-i\bar{\alpha})]. \tag{4.22}$$

Thus, by Eq. (3.10)

$$F^r(\mathbf{k},\bar{\alpha})=[E(\mathbf{k})-i\bar{\alpha}]^{-1}, \tag{4.23}$$

with

$$E(\mathbf{k})=\tfrac{1}{2}[J(\mathbf{0})-J(\mathbf{k})]-(1/N)\sum_{\mathbf{k}'} b_{\mathbf{k}'}^- \times(J(\mathbf{0})+J(\mathbf{k}-\mathbf{k}')-J(\mathbf{k}')-J(\mathbf{k})). \tag{4.24}$$

This is the usual Hartree-Fock spin-wave renormalization result,[8] in this case obtained by approximating $\Xi_{qq'}{}^r(\mathbf{k},\bar{\alpha})$ by $\Xi_{qq'}{}^r[\mathbf{k},\omega(\mathbf{k})]$ or self-consistently by $E(\mathbf{k})$.

The damping term is introduced into the first self-energy graph which has "dynamic" spin-wave contributions in the intermediate states as in Fig. 13(b) in distinction to Fig. 13(a), which only has a "static" intermediate spin wave. The equivalent self-energy diagram corresponding to Fig. 13(b) gives a self-energy contribution

$$[N^5/4(2N)^8\beta^2]\sum_{p_2p_3p_4} F(p_2)F(p_3)F(p_4)J^2(\mathbf{k})\cdots J^2(\mathbf{k}_4)\delta(p+p_2-p_3-p_4) \times\frac{[J(\mathbf{k}-\mathbf{k}_4)+J(\mathbf{k}_2-\mathbf{k}_4)-4B+2i\bar{\alpha}+2i\bar{\alpha}_2][J(\mathbf{k}_3-\mathbf{k})+J(\mathbf{k}_3-\mathbf{k}_2)+J(\mathbf{k}_4-\mathbf{k})+J(\mathbf{k}_4-\mathbf{k}_2)-8B+4i(\bar{\alpha}_3+\bar{\alpha}_4)]}{(B-i\bar{\alpha})^2(B-i\bar{\alpha}_2)^2(B-i\bar{\alpha}_3)^2(B-i\bar{\alpha}_4)^2}. \tag{4.25}$$

Instead of evaluating this rigorously, we shall make the low-temperature substitutions $i\bar{\alpha}_j=\omega(\mathbf{k}_j)$, which, in fact, violates the δ function on the frequencies $\delta(p_j)$.

Thus

$$\Xi(\mathbf{k},\bar{\alpha})=(1/N^3\beta^2)\sum_{p_2p_3} G(\mathbf{k},\mathbf{k}_2,\mathbf{k}_3)F(p_2)F(p_3)F(p+p_2-p_3), \tag{4.26}$$

where

$$G(\mathbf{k},\mathbf{k}_2,\mathbf{k}_3)=\tfrac{1}{2}[J(\mathbf{k})+J(\mathbf{k}_2)-J(\mathbf{k}_3-\mathbf{k}_2)-J(\mathbf{k}_3-\mathbf{k})][J(\mathbf{k}_3)+J(\mathbf{k}+\mathbf{k}_2-\mathbf{k}_3)-J(\mathbf{k}_3-\mathbf{k})-J(\mathbf{k}_3-\mathbf{k}_2)]. \tag{4.27}$$

The final result for the damped spin wave, in this approximation, is

$$F^d(\mathbf{k}, \bar{\alpha}) = [E(\mathbf{k}) - i\bar{\alpha} - \Xi^d(\mathbf{k}, \bar{\alpha})]^{-1}, \tag{4.28}$$

with

$$\Xi^d(\mathbf{k}, \bar{\alpha}) = \frac{1}{N^2} \sum_{\mathbf{k}_2\mathbf{k}_3} \frac{G(\mathbf{k}; \mathbf{k}_2, \mathbf{k}_3) M(\mathbf{k}; \mathbf{k}_2, \mathbf{k}_3; \beta)}{E(\mathbf{k}_3) + E(\mathbf{k}+\mathbf{k}_2-\mathbf{k}_3) - E(\mathbf{k}_2) - i\bar{\alpha}}, \tag{4.29}$$

where

$$M(\mathbf{k}; \mathbf{k}_2\, \mathbf{k}_3; \beta) = b^-(\mathbf{k}_3)[b^-(\mathbf{k}_2) - b^-(\mathbf{k}+\mathbf{k}_2-\mathbf{k}_3)] + b^-(\mathbf{k}_2) b^+(\mathbf{k}+\mathbf{k}_2-\mathbf{k}_3),$$

where we have used the renormalized notation $b^-(\mathbf{k}) = [\exp\beta E(\mathbf{k}) - 1]^{-1}$. In terms of the analytically continued values $i\bar{\alpha} = \omega + is$, with $s \to 0^+$, we obtain the results of Tahir-Kheli and ter Haar,[10] for the damping coefficient $\gamma(\mathbf{k}, \omega)$ and the real shift $R(\mathbf{k}, \omega)$,

$$\Xi^d(\mathbf{k}, \omega \pm is) = R(\mathbf{k}, \omega) \pm i\gamma(\mathbf{k}, \omega). \tag{4.30}$$

The results in this section well illustrate the ideal spin-wave methods of Dyson and others.[9] The T^4 contribution to the free energy is obtained from the Dyson form of the Heisenberg model by considering only the first-order terms in the interaction operator.

Thus, in terms of the ideal spin-wave boson operators $a_\mathbf{k}$ and $a_\mathbf{k}^\dagger$, the interaction Hamiltonian is

$$H_1^{\text{Dyson}} = (1/4N) \sum_{\mathbf{k}\mathbf{k}'\mathbf{q}} \Gamma(\mathbf{k}\mathbf{k}'\mathbf{q})\, a_\mathbf{k}^\dagger a_{\mathbf{k}'}^\dagger a_{\mathbf{k}-\mathbf{q}} a_{\mathbf{k}'+\mathbf{q}}, \tag{4.31}$$

with $\Gamma(\mathbf{k}\mathbf{k}'\mathbf{q}) = J(\mathbf{k}) + J(\mathbf{k}') - 2J(\mathbf{q})$. So

$$\Delta F^{\text{Dyson}} = (1/4N) \sum_{\mathbf{k}\mathbf{k}\mathbf{q}} \Gamma(\mathbf{k}\mathbf{k}'\mathbf{q}) \times \langle a_\mathbf{k}^\dagger a_{\mathbf{k}'}^\dagger a_{\mathbf{k}-\mathbf{q}} a_{\mathbf{k}'+\mathbf{q}} \rangle_{\text{spin waves}} \tag{4.32}$$

or

$$\Delta F^{\text{Dyson}} = (1/2N) \sum_{\mathbf{k}\mathbf{k}'} b_\mathbf{k}^- b_{\mathbf{k}'}^- \times [J(\mathbf{k}) + J(\mathbf{k}') - J(\mathbf{k}-\mathbf{k}') - J(\mathbf{0})]. \tag{4.33}$$

This is identical with Eq. (4.18). The correspondence occurs because of the method of representing "Bose-like" operators $S^\pm$ by pairs of fermion operators. This necessitates 4th-order graphs (or their equivalent) in the present notation before spin-wave interactions can occur. Consequently one can always identify graphs in the present method with any resulting from spin-wave theory. The advantage of the present method is that it is well defined throughout the whole temperature regime (in distinction to spin-wave theory, which is strictly valid only at low temperatures,

$$\exp[-(\tfrac{1}{2})\beta J(\mathbf{0})] \ll 1,$$

as Dyson has shown). Moreover, the kinematic restrictions are built directly into the present theory through the dynamical nature (C and D fields) of the equivalent vertices and can, in principle, be evaluated at any finite temperature.

5. CONCLUSIONS

The Green's-function methods (derived in earlier papers) have been used to investigate the Heisenberg model of ferromagnetism incorporating all the standard diagrammatic techniques of quantum-field theory. The usual high-density classification carried out to zeroth and first order in $1/Z$ resulted in molecular-field and spin-wave theory, respectively. A low-temperature classification similar to that of Stinchcombe *et al.* has also been carried out, which extends the validity of the above high-density results throughout the whole temperature range and which systematically accounts for the kinematical effects of ideal spin-wave theory. Further terms introduced spin-wave scattering effects as the next important contribution to the free energy at low temperatures, and the cancellation of the T^3 term was demonstrated leaving Dyson's T^4 term in the first Born approximation. Higher-order terms in the interaction resulted in spin-wave renormalization and damping, which indicated the nature of the approximation in other methods, such as decoupling of the equations of motion. It is hoped that these effects will be evaluated at finite temperatures in a later paper.

ACKNOWLEDGMENTS

The author would like to express his gratitude for help and assistance offered by Dr. S. Doniach and for two very useful conversations with Dr. R. B. Stinchcombe.